THE JOURNAL OF BIOLOGICAL CHEMISTRY
Vol. 274, No. 51, Issue of December 17, pp. 36559–36564, 1999

Printed in U.S.A.

Single Amino Acid Substitutions in α-Conotoxin PnIA Shift Selectivity for Subtypes of the Mammalian Neuronal Nicotinic Acetylcholine Receptor*

(Received for publication, July 22, 1999, and in revised form, September 27, 1999)

Ron C. Hogg‡, Les P. Miranda§, David J. Craik§¶, Richard J. Lewis‡§, Paul F. Alewood§, and David J. Adams‡‖

From the ‡Department of Physiology and Pharmacology and §Centre for Drug Design and Development, University of Queensland, Brisbane, Queensland 4072, Australia

The α-conotoxins, a class of nicotinic acetylcholine receptor (nAChR) antagonists, are emerging as important probes of the role played by different nAChR subtypes in cell function and communication. In this study, the native α-conotoxins PnIA and PnIB were found to cause concentration-dependent inhibition of the ACh-induced current in all rat parasympathetic neurons examined, with IC_{50} values of 14 and 33 nM, and a maximal reduction in current amplitude of 87% and 71%, respectively. The modified α-conotoxin [N11S]PnIA reduced the ACh-induced current with an IC_{50} value of 375 nM and a maximally effective concentration caused 91% block. [A10L]PnIA was the most potent inhibitor, reducing the ACh-induced current in ~80% of neurons, with an IC_{50} value of 1.4 nM and 46% maximal block of the total current. The residual current was not inhibited further by α-bungarotoxin, but was further reduced by the α-conotoxins PnIA or PnIB, and by mecamylamine. ^{1}H NMR studies indicate that PnIA, PnIB, and the analogues, [A10L]PnIA and [N11S]PnIA, have identical backbone structures. We propose that positions 10 and 11 of PnIA and PnIB influence potency and determine selectivity among α7 and other nAChR subtypes, including α3β2 and α3β4. Four distinct components of the nicotinic ACh-induced current in mammalian parasympathetic neurons have been dissected with these conopeptides.

Conotoxins are cysteine-rich peptides from the venom of the predatory marine snail of the genus *Conus*. These toxins are classified according to their primary structure and biological activity and include the α-conotoxin class, which possess a two-loop framework containing two disulfide bonds and are specific inhibitors of nicotinic acetylcholine receptors (nAChRs).[1] Native neuronal nAChRs are composed from a number of distinct subunits (α2–α7 and α9; β2–β4), which combine to form functional receptors showing a range of pharmacological properties. PnIA and PnIB[2] are 16-residue peptides isolated from the venom of the molluscivorous *Conus pennaceus* that differ by two amino acids at positions 10 and 11 (see Table I). PnIA and PnIB were originally reported to block ACh-evoked responses in *Aplysia* neurons (1) and, more recently, to exhibit activity in bovine adrenal chromaffin cells, but not at the mammalian neuromuscular junction (2).

The x-ray crystal structures of both PnIA (6) and PnIB (7) are similar, comprising an α-helix between residues 5 and 12, a 3_{10} helical turn at the N terminus, and consecutive β-turns at the C terminus. In both structures, the side chains of residues 10 and 11 are exposed on the surface of the molecules and hence mutation of these residues would not be expected to produce significant changes in the global fold. Data obtained from ^{1}H NMR experiments in the current study confirm this is indeed the case. The high degree of surface exposure of these residues and their lack of structural perturbation means that changes in activity among these peptides can be correlated directly to different residue side chains having different binding interactions at different nAChR subtypes.

Preliminary studies have shown that PnIA and PnIB differentially inhibit the nicotine-induced catecholamine release from bovine chromaffin cells (2). Differences in potency must be due to the residues at positions 10 and 11 of these conotoxins. Position 10 is of particular interest as this position typically contains different hydrophobic residues in other neuronal nAChR-selective conotoxins, EpI (3), MII (4), and ImI (5). To further elucidate the role of the residues at positions 10 and 11 in conferring nAChR subtype selectivity, the modified toxins [A10L]PnIA and [N11S]PnIA (see Table I) were synthesized. The aim of this study was to determine the selectivity of both the native and modified α-conotoxins PnIA and PnIB for the different nAChR subtypes, which constitute the whole-cell ACh-induced current in mammalian peripheral neurons, and to provide information as to the relative contribution of these nAChR subunits to the whole-cell response. These studies reveal significant differences in the selectivity and potency of PnIA and PnIB that arise through a key mutation at position 10 of these α-conotoxins.

EXPERIMENTAL PROCEDURES

Materials for Conotoxin Synthesis—N-Boc-L-amino acids and reagents used during chain assembly were peptide synthesis grade pur-

* This work was supported in part by an Australian Research Council grant (to D. J. A. and R. J. L.) and a National Health and Medical Research Council of Australia grant (to D. J. A.). The costs of publication of this article were defrayed in part by the payment of page charges. This article must therefore be hereby marked "*advertisement*" in accordance with 18 U.S.C. Section 1734 solely to indicate this fact.

¶ Australian Research Council senior fellow.

‖ To whom correspondence should be addressed: Dept. of Physiology and Pharmacology, University of Queensland, Brisbane, Queensland 4072, Australia. Fax: 61-7-3365-4933; E-mail: dadams@plpk.uq.edu.au.

[1] The abbreviations used are: nAChR, nicotinic acetylcholine receptor; ACh, acetylcholine; HATU, *O*-(7-aza-benzotriazol-1-yl)-1,1,3,3-tetramethyluronium hexafluorophosphate; HPLC, high pressure liquid chromatography; TOCSY, total correlation spectroscopy; NOESY, nuclear Overhauser spectroscopy; IC_{50}, half-maximal inhibitory concentration; RP, reverse phase; Boc, butoxycarbonyl.

[2] Native α-conotoxins PnIA and PnIB most likely contain a post-translationally modified sulfotyrosine 15 residue (J. Gehrmann, unpublished observation); however, the unsulfated forms [Tyr^{15}]PnIA and [Tyr^{15}]PnIB originally described (1) were used in the present study. The activities of the related α-conotoxin EpI and its unsulfated analogue [Tyr^{15}]EpI have been shown to be similar (3).

chased from Auspep (Melbourne, Australia) and Novabiochem (San Diego, CA). *N*-Boc-(L)-amino acid-phenylacetamidomethyl resin and 4-methylbenzylhydrylamine resin were purchased from Applied Biosystems (Foster City, CA) and the Peptide Institute (Osaka, Japan), respectively. Anhydrous dimethyl sulfoxide (Me_2SO), *p*-cresol, *p*-thiocresol, and resorcinol were purchased from Aldrich (Sydney, Australia). 2-(1*H*-Benzotriazol-1-yl)-1,1,3,3-tetramethyluronium hexafluorophosphate was purchased from Richelieu Biotechnologies (Quebec, Canada) and *O*-(7-aza-benzotriazol-1-yl)-1,1,3,3-tetramethyluronium hexafluorophosphate (HATU) was prepared as described previously (8, 9). Screw-cap glass peptide synthesis reaction vessels (4 ml) with sintered glass filter frit (10) were obtained from Embell Scientific Glassware (Queensland, Australia). Anhydrous hydrogen fluoride was purchased from Matheson Gas (BOC Gases, Melbourne, Australia).

Solid-phase Peptide Synthesis—The chain assemblies of [A10L]PnIA and [N11S]PnIA were carried using HATU/dimethyl formamide coupling chemistry as described previously (11). The following amino acid side-chain protection was used: Boc-Asn(xanthyl)-OH, Boc-Asp(*O*-cyclohexyl)-OH, Boc-Cys(4-methylbenzyl)-OH, Boc-Boc-Ser(*O*-benzyl)-OH, and Boc-Tyr(2-bromobenzyloxycarbonyl)-OH. Following chain assemblies, the peptide resins were cleaved with hydrogen fluoride/*p*-cresol/*p*-thiocresol (18:1:1, v/v) at 0 °C for 1.5 h. After evaporation of the hydrogen fluoride, the crude peptide was precipitated and washed with cold anhydrous diethyl ether (2 × 10 ml), dissolved in 50% aqueous acetonitrile, and lyophilized after aqueous dilution. The crude lyophilized peptide was reconstituted in 50% acetonitrile and then analyzed by reversed-phase high pressure liquid chromatography (RP-HPLC) and electron spray mass spectrometry.

HPLC—Analytical RP-HPLC was performed with a Waters 600E solvent delivery system. Data were collected by using a 484 absorbance detector (Applied Biosystems) at 214 nm. Chromatographic separations were achieved with a 1%/min linear gradient of buffer B in A (A = 0.1% trifluoroacetic acid in H_2O; B = 90% CH_3CN, 10% H_2O, 0.09% trifluoroacetic acid) over 80 min at a flow rate of 1 ml/min and 8 ml/min using Vydac C18 analytical (5 μm, 0.46 × 25 cm) and preparative C18 (10 μm, 2.2 × 25 cm) columns, respectively.

Electron Spray Mass Spectrometry—Mass spectra were acquired on a PE-Sciex API-III triple quadrupole mass spectrometer equipped with an Ionspray atmospheric pressure ionization source. Samples (typically 10 μl) were injected into a moving solvent (30 μl/min; 1:1 CH_3CN/0.05% trifluoroacetic acid in H_2O) coupled directly to the ionization source by a fused silica capillary interface (50 μm inner diameter × 50 cm length). Sample droplets were ionized at a positive potential of 5 kV and entered the analyzer through an interface plate and subsequently through an orifice (100–120 μm in diameter) at a potential of 80–100 V. Full scan mass spectra were acquired over the mass range of 500–2000 Da with a scan step size of 0.2 Da. Molecular masses were derived from the observed m/z values by using MACSPEC 3.3 software (PE-Sciex, Toronto, Canada). Theoretical monoisotopic and average masses were calculated by using the MacBiospec program (PE-Sciex).

Folding of [A10L]PnIA and [N11S]PnIA—Air oxidations were carried out by dissolving 10 mg of the lyophilized crude [A10L]PnIA or [N11S]PnIA crude cleavage material in 45 ml of 1:1 0.1 M NH_4HCO_3/isopropyl alcohol (pH 8.25) with vigorous stirring at room temperature for 1 h. Prior to purification the solution was acidified to pH 3 with trifluoroacetic acid and analyzed by analytical C4 RP-HPLC using a linear gradient of 0–80% B at 1%/min while monitoring by UV absorbance at 214 nm and electron spray mass spectrometry. Oxidized [A10L]PnIA was then purified by semipreparative HPLC using the same chromatographic conditions in 27% and 32%, yield. The sequences of the native and modified α-conotoxins used in the present study are shown in Table I.

Cell Preparation—Parasympathetic neurons from juvenile (2–4 weeks old) rat intracardiac ganglia were isolated and cultured as described previously (12). Briefly, rats were killed by decapitation, the hearts were excised, and the atria were removed and incubated for ~1 h at 37 °C in a saline solution, containing 1 mg/ml collagenase (type 2, Worthington) and 0.35 mg/ml trypsin (type III). Following enzymatic treatment, clusters of ganglia were dissected from the epicardial ganglion plexus, and neurons were dispersed by trituration in a high glucose culture medium (Dulbecco's modified Eagle's medium, containing 10% (v/v) fetal calf serum, 100 units/ml penicillin, and 0.1 mg/ml streptomycin). Dissociated neurons were plated on to laminin-coated glass coverslips and incubated at 37 °C in a 95% air, 5% CO_2 atmosphere for 24–72 h. For experimentation, coverslips containing dissociated neurons were transferred to a perfusion chamber (0.5 ml volume) mounted on an inverted microscope.

Electrophysiological Recording—Current and voltage recordings were made using the whole-cell recording configuration of the patch clamp technique. Electrical access to the cell interior was obtained using the perforated patch whole-cell recording configuration (13). The perforated patch configuration allows electrical access to the cell interior without the loss of cytoplasmic components, which is important in maintaining functional responses in these cells. A final concentration of 240 μg/ml amphotericin B in 0.4% Me_2SO was used in the pipette solution. Pipettes were pulled from thin walled borosilicate glass (Clark Electromedical Instruments, Reading, UK) and after fire polishing had resistances of ~1 MΩ. Access resistances using the perforated patch configuration were routinely 4–8 MΩ before series resistance compensation.

Membrane currents were recorded using an Axopatch 200A patch clamp amplifier (Axon Instruments Inc., Foster City, CA), filtered at 2–10 kHz, then digitized at 10–50 kHz (Digidata 1200 interface, Axon Instruments Inc.) and stored on the hard disc of a PC for viewing and analysis. Voltage and current protocols were applied using pClamp software (version 6.1.2, Axon Instruments Inc.). Dose-response curves were fitted using a Chi square minimization, non-linear curve fitting routine Microcal Origin 5.0 (Microcal Software Inc., Northampton, MA). Numerical data are presented as the mean ± S.E. (*n*, number of observations).

Solutions and Reagents—The pipette filling solution for perforated patch experiments contained (mM): 75 K_2SO_4, 55 KCl, 5 $MgSO_4$ and 10 HEPES, titrated with *N*-methyl-D-glucamine to pH 7.2. The control extracellular solution contained (mM): 140 NaCl, 3 KCl, 2.5 $CaCl_2$, 1.2 $MgCl_2$, 7.7 glucose, and 10 HEPES-NaOH. Acetylcholine (500 μM) and atropine (100 nM, to inhibit muscarinic ACh receptor activation), were applied for a duration of 2 s using a rapid piezo application system to overcome the rapid desensitization of the α7 component (14). Toxins were applied to the agonist solution as well as the constant perfusing solution. The time course of solution changes was <5 ms as determined from the change in junction potential upon switching from normal bath solution to one diluted with 2% deionized water. Experiments were carried out at 22 °C. The osmolality of all solutions was monitored with a vapor pressure osmometer (Westcor 5500) and was in the range 280–290 mOsmol. All chemicals used were of analytical grade. The following drugs were used: acetylcholine chloride, atropine hydrochloride, mecamylamine hydrochloride, cytisine, all supplied by Sigma.

NMR Spectroscopy—For NMR analysis, peptides were dissolved in 30% CD_3CN, 70% H_2O at a concentration of 1.0 mM as preliminary spectra of PnIA and PnIB recorded in pure H_2O suggested a degree of conformational averaging[3] in aqueous solution. ^1H NMR spectra were recorded at 283 K on a Bruker ARX 500 spectrometer. Total correlation spectroscopy (TOCSY) spectra (15) were recorded using a MLEV-17 spin lock sequence (16) with a mixing time of 80 ms, and nuclear Overhauser spectroscopy (NOESY) spectra (17) were recorded with a 200 ms mixing time. The water signal was suppressed in TOCSY and NOESY spectra using a modified WATERGATE sequence (18) in which two gradient pulses of 2-ms duration and 6 gauss cm^{-1} strength were applied either side of a binomial 3–9-19 pulse. Two-dimensional spectra were acquired over 6024 Hz and collected into 4096 data points with 512 t_1 increments of 32–64 scans. Spectra were processed on a Silicon Graphics Indy workstation using UXNMR (Bruker) software. Generally, data in both dimensions were multiplied by a sine-bell function shifted by 90° prior to Fourier transformation and a polynomial baseline correction applied to selected regions.

TABLE I
Sequences of native and modified α-conotoxins

Single-letter amino acid codes are used. Heavy lines between cysteine residues represent disulfide bonds.

Name	Sequence	Ref
PnIA	G CC S L P P C A A N NP D Y C - NH_2	(1)
[A10L]PnIA	G CC S L P P C A L N NP D Y C - NH_2	
[N11S]PnIA	G CC S L P P C A A S NP D Y C - NH_2	
PnIB	G CC S L P P C A L S NP D Y C - NH_2	(1)
EpI	G CC S D P R C N MN NP D Y C - NH_2	(3)
MII	G CC S N P V C H L E HS N L C - NH_2	(4)
ImI	G CC S D P R C A WR - - - - C - NH_2	(5)

[3] J. Gehrmann, personal communication.

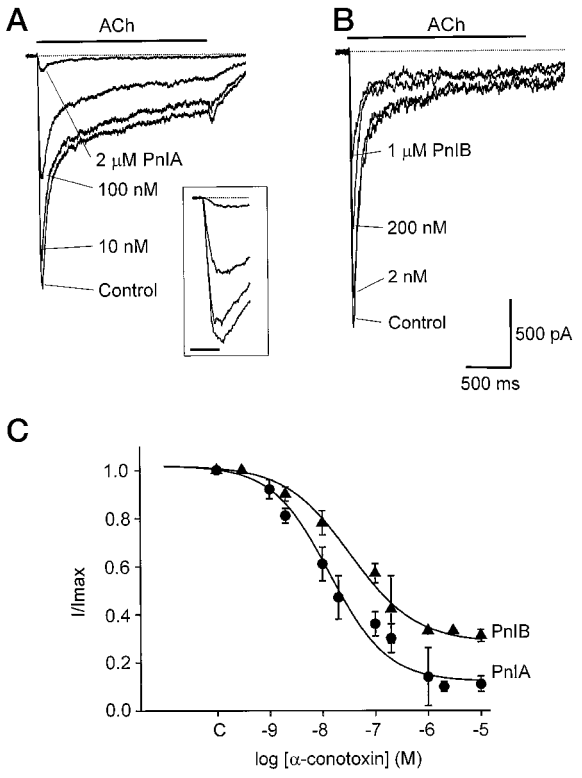

FIG. 1. **Effects of the native toxins, PnIA and PnIB, on the nicotinic ACh-evoked currents in rat intracardiac neurons.** Rapid application of 500 μM ACh in the presence of atropine (100 nM) evokes a characteristic biphasic response, with an initial peak which rapidly decays to a steady-state level. Superimposed traces of whole-cell ACh-induced currents in the absence (control) and presence of various concentrations of PnIA (*A*) and PnIB (*B*). *Inset*, peak currents from *A* shown on an expanded time scale. *Horizontal bar*, 50 ms. Inhibition of the steady-state current by the conotoxins examined was variable, hence, all measurements were of the peak current. Holding potential was −80 mV in *A*, and −70 mV in *B*. *C*, dose-response relationship obtained for the inhibition of the peak ACh-induced current by PnIA (●) and PnIB (▲). IC_{50} values obtained from curve fitting were 14 and 33 nM, respectively.

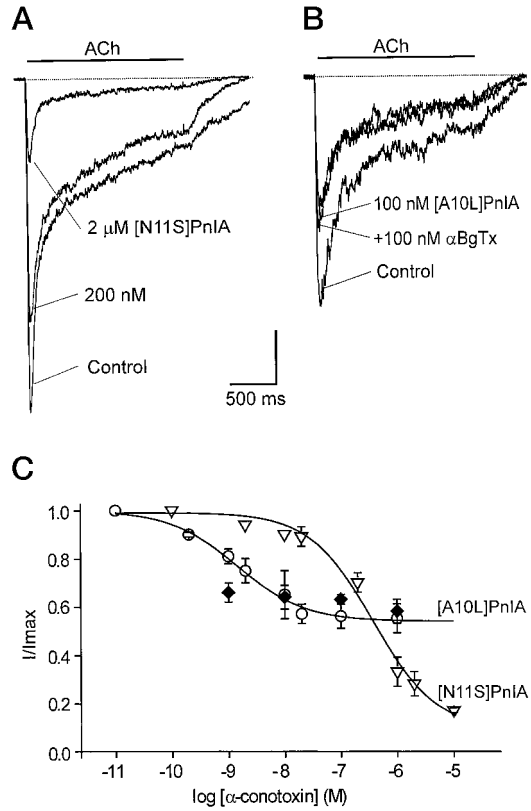

FIG. 2. **Effects of the modified α-conotoxins, [N11S]PnIA and [A10L]PnIA, on the ACh-evoked current in rat intracardiac neurons.** *A*, cumulative addition of 200 nM and 2 μM [N11S]PnIA reduces the ACh-evoked current in this neuron. Holding potential, −60 mV. *B*, 100 nM [A10L]PnIA blocks ~30% of the ACh-evoked current, and subsequent addition of 100 nM α-bungarotoxin does not cause further inhibition of the response. Holding potential, −90 mV. *Vertical bar* represents 0.5 nA in *A* and 0.2 nA in *B*. *C*, dose-response relationship for the inhibition of the peak nicotinic ACh-evoked current by [N11S]PnIA (▽) and [A10L]PnIA (○). IC_{50} values obtained from fits for [N11S]PnIA and [A10L]PnIA were 375 and 1.4 nM, respectively.

RESULTS

Rapid focal application of 500 μM ACh to dissociated rat intracardiac ganglion neurons, in the presence of 100 nM atropine, resulted in a characteristic biphasic inward current comprising an initial transient peak which rapidly decayed to a steady-state current (Fig. 1, *A* and *B*). The ratio of peak to steady-state current amplitude varied between neurons, which may be attributable to the heterogeneous mRNA expression of different nAChR subunits reported in rat intracardiac neurons (19). The peak whole-cell ACh-evoked current in all neurons was reversibly inhibited >95% by 1 μM mecamylamine (data not shown), a non-selective nicotinic AChR antagonist (12). Since inhibition of the steady-state current by the α-conotoxins examined was variable, all measurements describe the inhibition of peak current. α-Conotoxin PnIA inhibited the ACh-induced current in a concentration-dependent manner (Fig. 1*A*), with an IC_{50} of 14 nM. PnIA did not completely inhibited the peak current, producing maximal reduction in amplitude of 87 ± 2% (n = 6) at a concentration of 10 μM (Fig. 1*C*). α-Conotoxin PnIB was less potent than PnIA, inhibiting the peak ACh-induced current (Fig. 1*B*) with an IC_{50} value of 33 nM (Fig. 1*C*). PnIB also did not completely block the peak nicotinic current, with a concentration of 10 μM, causing a maximum reduction of only 68 ± 3% (n = 5) (Fig. 1*C*). PnIA and PnIB were each effective at reducing ACh-induced current in all neurons examined.

The potency of two substituted α-conotoxins [A10L]PnIA and [N11S]PnIA to block the nicotinic ACh-induced current was also examined. [N11S]PnIA was the least potent inhibitor of the ACh-induced current in these neurons, having an IC_{50} of 375 nM, with 17 ± 1% (n = 4) of the current resistant to 10 μM [N11S]PnIA (Fig. 2*A*). A plateau was not reached in the dose-response relationship, but the fitted curve predicts a maximum inhibition of 91% (Fig. 2*C*), similar to that achieved with PnIA. Higher concentrations were not tested due to limited availability of the toxin. [N11S]PnIA was effective in reducing the ACh-induced current in all neurons examined. In contrast, [A10L]PnIA was the most potent of the α-conotoxins examined. However, the nicotinic ACh-induced current in ~20% of neurons was insensitive to block by [A10L]PnIA. The IC_{50} value for the [A10L]PnIA-sensitive component of the current was 1.4 nM, with 56 ± 6% (n = 4) of the total nicotinic ACh-induced current insensitive to block by [A10L]PnIA (Fig. 2*C*). The current remaining in the presence of a maximally effective concentration of [A10L]PnIA was not inhibited further by α-bungarotoxin (Fig. 2*B*), a selective inhibitor of neuronal nAChRs containing the α7 subunit (20), but could be further reduced by either 200 nM EpI, which selectively inhibits receptors containing α3β2 and α3β4 subunits (3), or 200 nM PnIA (data not shown). In cells insensitive to [A10L]PnIA, the peak current could be inhibited by EpI (200 nM) (Fig. 3*A*) or PnIA.

α-Bungarotoxin inhibited the nicotinic ACh-induced current in ~80% of neurons examined, and these results are included

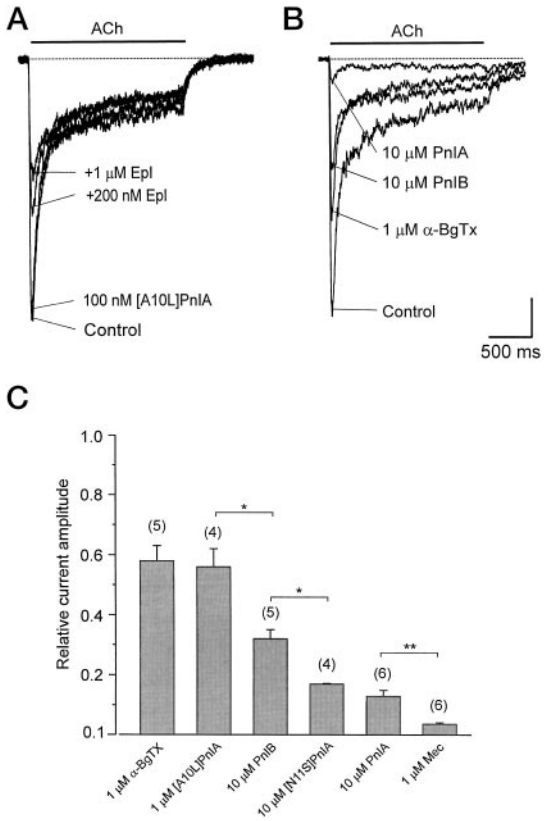

FIG. 3. **Effect of α-conotoxins and α-bungarotoxin on ACh-evoked currents.** *A*, [A10L]PnIA did not affect the ACh-evoked current in this cell; however, subsequent application of 200 nM EpI inhibited the current amplitude by ~50% (see Ref. 21). Holding potential, −70 mV. *B*, progressive inhibition of the ACh-evoked current by cumulative addition of saturating concentrations of α-bungarotoxin, PnIB and PnIA. Holding potential, −80 mV. *Vertical bar* represents 0.5 nA in *A* and 0.3 nA in *B*. *C*, bar graph of the relative inhibition of the nicotinic ACh-evoked current amplitude (mean ± S.E.) at maximally effective concentrations of PnIA, [A10L]PnIA, [N11S]PnIA, PnIB, α-bungarotoxin, and mecamylamine. *, $p < 0.005$; **, $p < 0.0005$.

in Fig. 3*C* for comparison. The residual peak current remaining following application of 1 μM α-bungarotoxin (58 ± 5% of control, $n = 5$), was not significantly different ($p > 0.25$) from the current resistant to 1 μM [A10L]PnIA (56 ± 6%, $n = 4$), and could be further inhibited by PnIB and PnIA (Fig. 3*B*). A comparison of the residual current amplitudes obtained in the presence of maximally effective concentrations of α-bungarotoxin, α-conotoxins, and mecamylamine are summarized in Fig. 3*C*.

To determine if PnIA can inhibit the α3β4 nAChR subtype, cytisine, which is more potent than ACh at activating the α3β4 receptor in a mammalian cell line (21), was used to activate whole-cell currents. PnIA (1 μM) inhibited the current evoked by cytisine (300 μM) by 37 ± 5% ($n = 5$) (data not shown), but even at a concentration of 10 μM, PnIA blocked a smaller proportion of the cytisine-evoked current than the ACh-evoked current. The residual cytisine-induced current reflects an increased contribution of a PnIA-insensitive nAChR subtype to the whole-cell current in rat intracardiac neurons.

To accurately interpret the observed changes in activity of the PnIA mutants, it was necessary to establish whether the substitutions at positions 10 and 11 produced any changes to the backbone structure of these peptides. Two-dimensional TOCSY and NOESY ^{1}H NMR spectra were recorded for the peptides and were assigned using standard methods, as described for the related α-conotoxin GI (22). Briefly, the TOCSY spectra were used to correlate peaks to particular amino acid

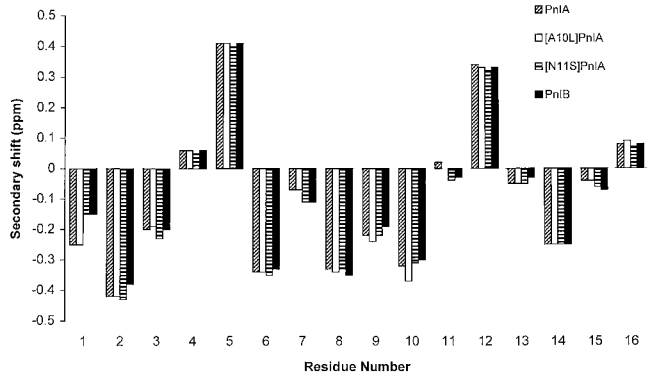

FIG. 4. **Secondary αH chemical shifts, *i.e.* differences between observed chemical shifts and random coil shifts, for PnIA, [A10L]PnIA, [N11S]PnIA, and PnIB.** The different mutants are identified by their amino acids at positions 10 and 11; the sequences at all other positions are identical. The random coil shifts used include corrections for residues preceding Pro in the sequence (24).

types and the NOESY spectra were used to delineate the sequence specific location of these amino acids (23). Secondary chemical shifts were then calculated by subtracting random coil shifts (24) from the αH chemical shifts for each of the constituent residues in the four peptides. These secondary shifts are highly diagnostic of local structural elements (24). Fig. 4 shows that the secondary shifts are almost identical for all four peptides, suggesting that the structures are similar. Further, the pattern of secondary shifts is consistent with the overlapping three-dimensional structures of PnIA and PnIB observed in the crystalline state derived by x-ray methods (6, 7). In particular, the pattern of negative secondary shifts in the middle section of all four peptides is consistent with the reported α-helix between residues 5 and 12 in PnIA and PnIB.

DISCUSSION

In contrast to a previous study, which found no activity of intracerebral injections of PnIA or PnIB into rat brain (1), the native α-conotoxins PnIA and PnIB both inhibit the nicotinic ACh-induced whole-cell current in rat intracardiac ganglion neurons in a dose-dependent manner. PnIA was 3-fold more potent and able to inhibit ~90% of the ACh-induced current at a maximally effective concentration, compared with ~70% for PnIB. The modified toxin [N11S]PnIA was an order of magnitude less potent than PnIB but also caused maximal inhibition of ~90%. [A10L]PnIA was an order of magnitude more potent than PnIA (IC_{50} of 1.4 nM) but caused a maximal inhibition of only ~45% of the peak current. The inhibition of ACh-evoked currents by native (PnIA, PnIB) and modified α-conotoxins ([A10L]PnIA, [N11S]PnIA) are summarized in Table II. Hill coefficients obtained from fits of the inhibitory dose-response curves were consistently less than unity, the significance of which is unclear, but are similar to those obtained for inhibition of α3β2 and α7 receptors expressed in oocytes by the α-conotoxins, MII (4) and ImI (26), respectively.

Previous studies have demonstrated that ~80% of rat intracardiac neurons express α7 subunits, based on the sensitivity of the whole-cell ACh-induced current to α-bungarotoxin (25) and mRNA expression of the α7 subunit (19). The IC_{50} value of 0.12 nM for α-bungarotoxin inhibition of the ACh-induced current obtained in rat intracardiac neurons (25) is more than 4 orders of magnitude lower than that obtained from α7 homomers expressed in *Xenopus* oocytes (26) suggesting that the native α7 receptors are not α7 homomers. In this study, bath application of α-bungarotoxin (1 μM) produced a maximal inhibition (42 ± 5%) that was similar to that obtained previously in rat intracardiac neurons (47 ± 2%) (25), and similar to the maximal

TABLE II
Inhibition of ACh-evoked current amplitude by α-conotoxins

Hill coefficients and percentage of maximal inhibition (± 95% confidence limits) were calculated from the fitted curve ("Experimental Procedures"). *n* represents number of data points to obtain the dose-response relationships.

Conotoxin	IC_{50}	Hill coefficient	Maximal inhibition	*n*
	nM		%	
PnIA	14	0.80	87 ± 2	41
[A10L]PnIA	1.4	0.71	46 ± 2	33
[N11S]PnIA	375	0.78	91 ± 3	24
PnIB	33	0.67	71 ± 3	32

inhibition seen in the present study with [A10L]PnIA. Furthermore, inhibition of the whole-cell current by α-bungarotoxin and [A10L]PnIA was not additive, suggesting that [A10L]PnIA and α-bungarotoxin selectively inhibit the same α7 component in these neurons. The potency and selectivity of conotoxin [A10L]PnIA make it the best conotoxin-derived pharmacological probe for α7 receptors. Previous studies on α-conotoxin ImI have suggested that the major binding determinants for the α7 receptor are found in the first loop (Asp^5-Pro^6-Arg^7) with an additional contribution to binding made by Trp^10 in the second loop (22, 28). Inspection of the primary (see Table I) and tertiary structures of [A10L]PnIA and ImI suggest that conotoxin [A10L]PnIA most likely binds at a different "microsite." More detailed structure-function studies will be required to determine the precise nature and site of interaction of [A10L]PnIA with the α7 receptor.

The α-conotoxin EpI isolated from *Conus episcopatus* has been shown previously to block α3β2 and α3β4 nicotinic receptors in rat intracardiac ganglion neurons (3). Both EpI and PnIA are able to further reduce the nicotinic ACh-induced current in the presence of a maximal concentration of [A10L]PnIA or α-bungarotoxin. [A10L]PnIA does not cause further block of either the ACh- or cytisine-evoked current in the presence of 1 μM PnIA ($n = 3$, data not shown), indicating that PnIA blocks the α7 component as well as additional components of the nAChR-mediated current in these neurons. The ACh-induced current in all cells was inhibited ~90% by [N11S]PnIA, suggesting that substitution of asparagine at position 11 for serine does not affect PnIA subtype selectivity, despite a ~30-fold reduction in potency. The results with [A10L]PnIA suggest that position 10 has an important influence on selectivity, with the larger, more hydrophobic leucine conferring selectivity for the α7 subunit of the nAChR and increased potency.

The NMR data clearly confirm that the changes in potency and selectivity brought about by mutations at positions 10 and 11 are not due to structural changes. αH secondary NMR chemical shifts provide a very sensitive fingerprint of both local and global structural change and confirm that the backbone structures are identical. The signs and magnitudes of the secondary shifts show that, like PnIA and PnIB, both mutants possess an α-helix between residues 5 and 12. The highly conserved nature of this helix upon substitution contrasts with the variation in the nature and extent of the helix when the number of amino acids between conserved cysteine residues is changed, as seen from our recent structural studies on conotoxins MII (29), GI (22), and ImI (30). Inspection of the crystal structures of PnIA and PnIB shows that residues 10 and 11 are both on the face of the helix exposed to the solvent, rather than packed toward the disulfide core of the peptides (see Fig. 5). The high surface exposure favors direct interactions of these residues with complementary binding sites on nAChRs. The larger hydrophobic surface at residue 10 in [A10L]PnIA is

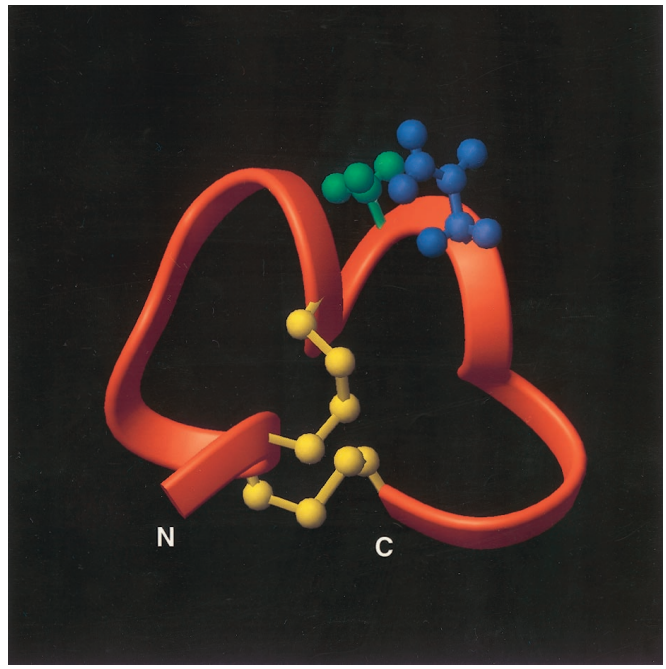

FIG. 5. **Ribbon representation of the α-conotoxin PnIA structure (6) showing the location of amino acid residues 10 (Ala; *green*) and 11 (Asn; *blue*) on the exposed face of the helix backbone (*red*).** The disulfide bonds connecting Cys^2–Cys^8 and Cys^3–Cys^{16} are shown in *yellow*.

presumably complementary with binding to the α7, but unfavorable for binding to the other subunit combinations in these neurons.

Although nAChRs are widely expressed throughout the vertebrate nervous system (31), their precise function in many cases is poorly understood. Neuronal nAChRs containing the α7 subunit have been identified in chick sympathetic neurons (32), rat hippocampal neurons (33), and chick ciliary ganglion (34). However, the physiological role of the α7 component in many of these systems remains unclear. Presynaptic nAChRs containing the α7 subunit have been shown to modulate neurotransmitter release (35, 36), and there is evidence that the receptors containing the α7 subunit are involved in synaptic transmission in chick ciliary ganglia (37). The α7 subunit does not appear to form functional postsynaptic nAChRs in rat parasympathetic neurons, as synaptic transmission in the rat submandibular ganglion is not affected by either α-bungarotoxin (1 μM) or [A10L]PnIA. Bath application of PnIA (1 μM), however, causes partial inhibition of synaptic transmission in rat parasympathetic ganglia, reducing excitatory postsynaptic potential amplitude by approximately 35%.[4]

The range of selectivities of native and modified α-conotoxins PnIA and PnIB for mammalian nAChRs makes these peptides valuable new tools for investigating the subunit composition of neuronal nAChRs at a functional level. At a molecular level, their small size lends them to relatively easy synthesis and modification and makes them ideal tools for investigating the structure function relationship of the subunits, which constitute neuronal nAChRs. This study shows the importance of individual α-conotoxin residues for defining both affinity and selectivity. With the four peptides investigated, it was possible to dissect four pharmacologically distinct nAChR-mediated currents, including a component mediated by nAChRs containing α7 subunits in rat intracardiac ganglion neurons. The nAChR subunit combinations giving rise to the other three

[4] A. B. Smith and D. J. Adams, unpublished observations.

components of the ACh-evoked current in these neurons remain to be fully elucidated, but are likely to include different combinations of those α and β subunits identified previously in single cell reverse transcription-polymerase chain reaction studies (19).

Acknowledgments—We thank John Gehrmann for helpful comments and for providing unpublished data on chemical shifts of PnIA and PnIB in various solvents, and Dianne Alewood for conopeptide synthesis.

REFERENCES

1. Fainzilber, M., Hasson, A., Oren, R., Burlingame, A. L., Gordon, D., Spira, M. E., and Zlotkin, E. (1994) *Biochemistry* **33,** 9523–9529
2. Broxton, N., Down, J. G., Miranda, L., Alewood, P., and Livett, B. G. (1998) *Proc. Aust. Neurosci. Soc.* **9,** 128
3. Loughnan, M., Bond, T., Atkins, A., Cuevas, J., Adams, D. J., Broxton, N. M., Livett, B. G., Down, J. G., Jones, A., Alewood, P. F., and Lewis, R. J. (1998) *J. Biol. Chem.* **273,** 15667–15674
4. Cartier, G. E. C., Yoshikama, D., Gray, W. R., Luo, S., Olivera, B. M. and McIntosh, J. M. (1996) *J. Biol. Chem.* **271,** 7522–7528
5. McIntosh, J. M., Yoshikama, D., Mahe, E., Nielsen, D. B. Rivier, J. E., Gray, W. R., and Olivera, B. M. (1994) *J. Biol. Chem.* **269,** 16733–16739
6. Hu, S.-H., Gehrmann, J., Guddat, L. W., Alewood, P. F., Craik, D. J., and Martin, J. L. (1996) *Structure* **4,** 417–423
7. Hu, S.-H., Gehrmann, J., Alewood, P. F., Craik, D. J., and Martin, J. L. (1997) *Biochemistry* **36,** 11323–11330
8. Carpino, L. A. (December 3, 1996) U. S. Patent 5,580,981
9. Carpino, L. A. (1993) *J. Am. Chem. Soc.* **115,** 4397–4398
10. Schnölzer, M., Alewood, P., Jones, A., Alewood, D., and Kent, S. B. H. (1992) *Int. J. Pept. Protein Res.* **40,** 180–193
11. Miranda, L. P., and Alewood, P. F. (1999) *Proc. Natl. Acad. Sci. U. S. A.* **96,** 1181–1186
12. Fieber, L. A., and Adams, D. J. (1991) *J. Physiol.* **434,** 215–237
13. Rae, J., Cooper, K., Gates, P., and Watsky, M. (1991) *J. Neurosci. Methods* **37,** 15–26
14. Zhang, Z. W., Vijayaraghavan, S., and Berg D. K. (1994) *Neuron* **12,** 167–177
15. Braunschweiler, L., and Ernst, R. R. (1983) *J. Magn. Reson.* **53,** 521–528
16. Bax, A., and Davis, D. G. (1985) *J. Magn. Reson.* **65,** 355–360
17. Jeener, J., Meier, B. H., Bachmann, P., and Ernst, R. R. (1979) *J. Chem. Phys.* **71,** 4546–4553
18. Piotto, M., Saudek, V., and Sklenar, V. (1992) *J. Biomol. NMR* **2,** 661–665
19. Poth, K., Nutter, T. J., Cuevas, J., Parker, M. J., Adams, D. J., and Luetje, C. W. (1997) *J. Neurosci.* **17,** 586–596
20. Couturier, S., Bertrand, D., Matter, J.-M., Hernandez, M.-C., Bertrand, S., Millar, N., Valera, S., Barakas, T., and Ballivet, M. (1990) *Neuron* **5,** 847–856
21. Lewis, T. M., Harkness, P. C., Sivilotti, L. G., Colquhoun, D., and Millar, N. S. (1997) *J. Physiol.* **505,** 299–306
22. Gehrmann, J., Alewood, P. F., and Craik, D. J. (1998) *J. Mol. Biol.* **278,** 401–415
23. Wüthrich, K. (1986) *NMR of Proteins and Nucleic Acids*, Wiley-Interscience, New York
24. Wishart, D. S., Bigam, C. G., Holm, A., Hodges, R. S., and Sykes, B. D. (1995) *J. Biomol. NMR* **5,** 67–81
25. Cuevas, J., and Berg, D. K. (1998) *J. Neurosci.* **18,** 10335–10344
26. Johnson, D. S., Martinez, J., Elgoyhen, A. B., Heinemann, S. F., and McIntosh, M. J. (1995) *Mol. Pharmacol.* **48,** 194–199
27. Quiram, P. A., and Sine, S. M. (1998) *J. Biol. Chem.* **273,** 11007–11011
28. Servent, D., Thanh, H. L., Antil, S., Bertrand, D., Corringer, P.-J., Changeux, J.-P., and Ménez, A. (1998) *J. Physiol.* (*Paris*) **92,** 107–111
29. Hill, J. M., Oomen, C. J., Miranda, L. P., Bingham, J. P., Alewood, P. F., and Craik, D. J. (1998) *Biochemistry* **37,** 15621–15630
30. Gehrmann, J., Daly, N. L., Alewood, P. F., and Craik, D. J. (1999) *J. Med. Chem.* **42,** 2364–2372
31. Sargent, P. B. (1993) *Annu. Rev. Neurosci.* **16,** 403–443
32. Yu, C. R., and Role, L. W. (1998) *J. Physiol.* **509,** 651–665
33. Alkondon, M., and Albuquerque, E. X. (1993) *J. Pharmacol. Exp. Ther.* **265,** 1455–1473
34. Chiappinelli, V. A., and Giacobini, E. (1978) *Neurochem. Res.* **3,** 465–478
35. McGehee, D., Heath, M., Gelber, S., and Role, L. W. (1995) *Science* **269,** 1692–1697
36. Li, X., Rainnie, D. G., McCarley, R. W., and Greene, R. W. (1998) *J. Neurosci.* **18,** 1904–1912
37. Chang, K. T., and Berg, D. K. (1999) *J. Neurosci.* **19,** 3701–3710

Single Amino Acid Substitutions in α-Conotoxin PnIA Shift Selectivity for Subtypes of the Mammalian Neuronal Nicotinic Acetylcholine Receptor

Ron C. Hogg, Les P. Miranda, David J. Craik, Richard J. Lewis, Paul F. Alewood and David J. Adams

J. Biol. Chem. 1999, 274:36559-36564.
doi: 10.1074/jbc.274.51.36559